

Extending Machine Learning Classification Capabilities with Histogram Reweighting

Dimitrios Bachtis,^{1,*} Gert Aarts,^{2,†} and Biagio Lucini^{1,3,‡}

¹*Department of Mathematics, Swansea University, Bay Campus, SA1 8EN, Swansea, Wales, UK*

²*Department of Physics, Swansea University, Singleton Campus, SA2 8PP, Swansea, Wales, UK*

³*Swansea Academy of Advanced Computing, Swansea University, Bay Campus, SA1 8EN, Swansea, Wales, UK*

(Dated: April 29, 2020)

We propose the use of Monte Carlo histogram reweighting to extrapolate predictions of machine learning methods. In our approach, we treat the output from a convolutional neural network as an observable in a statistical system, enabling its extrapolation over continuous ranges in parameter space. We demonstrate our proposal using the phase transition in the two-dimensional Ising model. By interpreting the output of the neural network as an order parameter, we explore connections with known observables in the system and investigate its scaling behaviour. A finite size scaling analysis is conducted based on quantities derived from the neural network that yields accurate estimates for the critical exponents and the critical temperature. The method improves the prospects of acquiring precision measurements from machine learning in physical systems without an order parameter and those where direct sampling in regions of parameter space might not be possible.

I. INTRODUCTION

Machine learning has recently emerged as an omnipresent tool across a vast number of research fields. A major milestone towards its wide success has been the unprecedented capability of deep neural networks to automatically extract hierarchical structures in data [1]. Historical implementations of machine learning revolved around problems in image recognition and natural language processing but recent advances have encompassed the physical sciences [2]. For a short review of machine learning for quantum matter see Ref. [3].

On the forefront of modern approaches, there have been significant contributions in the realm of computational physics. Notably, machine learning was employed to study phase transitions in classical and quantum many-body systems [4]. The aim is typically the separation of phases in a system by relying on supervised, unsupervised or semi-supervised learning of its configurations. A variety of algorithms including convolutional neural networks, support vector machines and principal component analysis have been implemented to achieve this goal [5–33]. Within these approaches, the Ising model, due to its simplicity, analytical solution [34], and non-trivial phase structure, frequently acts as a prototypical testing ground to demonstrate results.

In addition, efficient Monte Carlo sampling was realized through the construction of effective Hamiltonians in physical systems [35–37]. Among these approaches, the self-learning Monte Carlo method was extended to continuous-time, quantum and hybrid Monte Carlo [38–48]. Deep reinforcement learning was utilized to generate ground states through the training of a machine learning agent [49], neural autoregressive models have

been applied within variational settings [50], and Boltzmann generators have been introduced to produce unbiased equilibrium samples in condensed-matter and protein systems [51]. In lattice field theories generative and regressive neural networks have been implemented [52], and sampling with flow-based methods has led to reduced autocorrelation times [53, 54].

Along these lines, there is an increasing need for tools that improve computational efficiency and simultaneously enable the extraction of more information from available machine learning predictions. The majority of machine learning implementations in related work obtain predictions on sets of data that have been acquired through a limited exploration of parameter space. This approach is restrictive and forbids the obtainment of precision measurements. Traditionally, in statistical mechanics, such obstacles are overcome by the use of Monte Carlo histogram reweighting techniques [55, 56]. It is then possible to acquire increased knowledge of observables by estimating them based on measurements from already conducted simulations. Furthermore, one can extrapolate in parameter space to glimpse into the behaviour of more complicated Hamiltonians. A proof of principle demonstration concerns reweighting from a zero external magnetic field to a non-zero value in the Ising model [55].

In this paper, we introduce histogram reweighting to supervised machine learning. In particular, we explore if the output from a neural network in a classification task can be treated as an observable in a statistical system and consequently be extrapolated to continuous ranges - providing a tool for further exploration without acquiring additional data and potentially even when direct sampling is not possible. We further interpret the output of the neural network as an effective order parameter within the context of a phase identification problem, and propose reweighting as a means to explore connections with standard thermodynamic observables of the system under consideration. Finally, we search for scaling behaviour in quantities derived from the machine learning

* dimitrios.bachtis@swansea.ac.uk

† g.aarts@swansea.ac.uk

‡ b.lucini@swansea.ac.uk

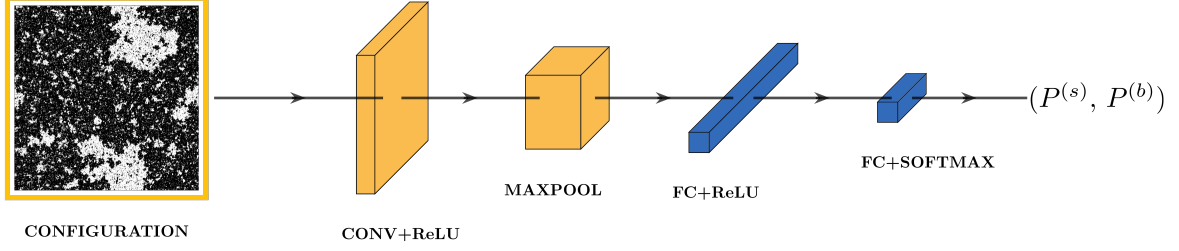


FIG. 1. The architecture of the convolutional neural network (see App. B). Importance-sampled configurations are presented as input to the neural network and are further processed through a series of transformations. The values of the output vector denote the probability that a configuration belongs in an associated phase. The probabilities are used as observables to be reweighted.

algorithm with an aim to study the infinite-volume limit of the statistical system.

To establish the method, we apply it to the two-dimensional Ising model, a system that undergoes a second-order phase transition from a broken-symmetry to a symmetric phase. Using our developments, we present an accurate calculation of the critical point and the critical exponents by relying exclusively on quantities derived from the machine learning implementation and their reweighted extrapolations.

II. HISTOGRAM REWEIGHTING

We consider a generic statistical system described by an action (or Hamiltonian) $S = \sum_k g^{(k)} S^{(k)}$, which separates in terms of a set of parameters $\{g^{(k)}\}$. During a Markov chain Monte Carlo simulation of the system we sample a representative subset of states $\sigma_1, \dots, \sigma_N$ based on a Boltzmann probability distribution:

$$p_{\sigma_i} = \frac{\exp[-\sum_k g^{(k)} S_{\sigma_i}^{(k)}]}{\sum_{\sigma} \exp[-\sum_k g^{(k)} S_{\sigma}^{(k)}]}, \quad (1)$$

where $Z = \sum_{\sigma} \exp[-\sum_k g^{(k)} S_{\sigma}^{(k)}]$ is the partition function and the sum is over all possible states σ in the system. The expectation value of an arbitrary observable O is then given by:

$$\langle O \rangle = \frac{\sum_{i=1}^N O_{\sigma_i} \tilde{p}_{\sigma_i}^{-1} \exp[-\sum_k g^{(k)} S_{\sigma_i}^{(k)}]}{\sum_{i=1}^N \tilde{p}_{\sigma_i}^{-1} \exp[-\sum_k g^{(k)} S_{\sigma_i}^{(k)}]}, \quad (2)$$

where \tilde{p}_{σ_i} are the probabilities used to sample configurations from the equilibrium distribution. We now consider the probabilities for a set of sufficiently adjacent parameter values $\{g_0^{(k)}\}$, given by:

$$p_{\sigma_i}^{(0)} = \frac{\exp[-\sum_k g_0^{(k)} S_{\sigma_i}^{(k)}]}{\sum_{\sigma} \exp[-\sum_k g_0^{(k)} S_{\sigma}^{(k)}]}. \quad (3)$$

After substituting \tilde{p}_{σ_i} with $p_{\sigma_i}^{(0)}$ in Eq. (2), we arrive at reweighting equation:

$$\langle O \rangle_{\{g^{(k)}\}} = \frac{\sum_{i=1}^N O_{\sigma_i} \exp[-\sum_k (g^{(k)} - g_0^{(k)}) S_{\sigma_i}^{(k)}]}{\sum_{i=1}^N \exp[-\sum_k (g^{(k)} - g_0^{(k)}) S_{\sigma_i}^{(k)}]}. \quad (4)$$

Given a series of Markov chain Monte Carlo measurements O_{σ_i} for a set of parameters $\{g_0^{(k)}\}$, Eq. (4) enables the calculation of expectation values for extrapolated sets of $\{g^{(k)}\}$. Successful extrapolations of observables should lie within ranges where the associated action histograms have markedly large values (e.g. see Ref. [57]).

III. REWEIGHTING OF MACHINE LEARNING OUTPUT

We employ reweighting techniques to study the phase transition in the two-dimensional Ising model (App. A) by formulating the phase identification task as a classification problem. We further investigate connections between the predicted classification label and known observables of the system. Finally, we perform a finite size scaling analysis to calculate critical exponents and the inverse critical temperature by relying exclusively on reweighted machine learning predictions.

We create the datasets using Markov chain Monte Carlo simulations with the Wolff algorithm [58]. The training data are comprised of a set of 1000 uncorrelated configurations at each training point, with 100 configurations chosen as a cross-validation set. The range of inverse temperatures chosen to generate configurations is $0.32, \dots, 0.41$ in the symmetric phase and $0.47, \dots, 0.56$ in the broken-symmetry phase with a step of 0.01. The ranges are chosen to be distant from the critical inverse temperature $\beta_c \approx 0.440687$. We train the convolutional neural network (CNN) for lattice sizes $L = 128, \dots, 760$. We implement the neural network architecture (App. B) with TensorFlow and the Keras library [59, 60]. The presence of a phase transition makes the convolutional neural

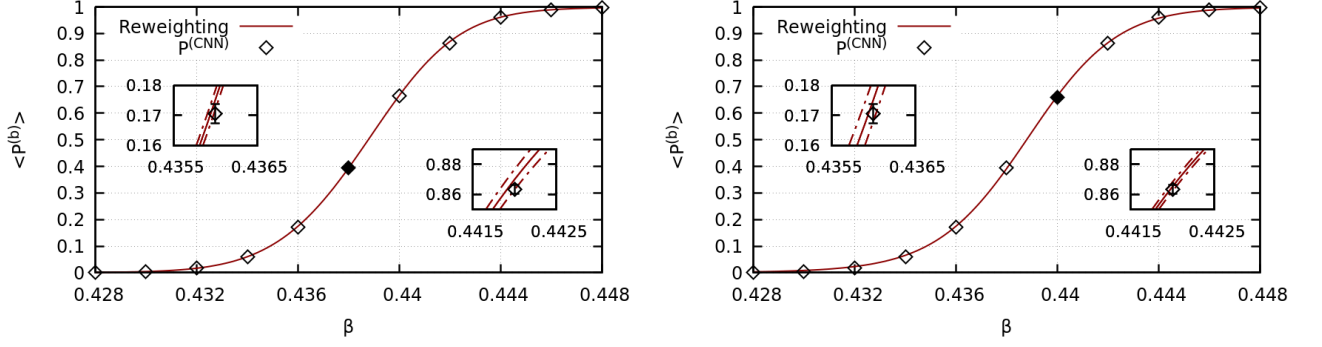


FIG. 2. Reweighting for the neural network output probability versus the inverse temperature of the 2D Ising model with lattice size $L = 128$. The reweighted extrapolations are depicted by the line. The filled point corresponds to the parameter choice $\beta_0 = 0.438$ (left) and $\beta_0 = 0.44$ (right) used to conduct reweighting. Empty points are actual predictions from the neural network on Monte Carlo datasets, added for comparison. The dashed lines, only visible in the insets, indicate the statistical uncertainty. The training was conducted for $\beta \leq 0.41$ and $\beta \geq 0.47$.

network a well suited choice to learn spatial dependencies across configurations in different phases.

After training is completed, we feed a configuration to the convolutional neural network to predict its associated classification label. The values of the output vector in the classification task sum up to one and are interpreted as the probability P_{σ_i} that a configuration σ_i belongs in the corresponding phase. When referring explicitly to the probabilities associated with the symmetric and the broken-symmetry phase we will denote them as $P_{\sigma_i}^{(s)}$ and $P_{\sigma_i}^{(b)}$, respectively, with $P_{\sigma_i}^{(s)} + P_{\sigma_i}^{(b)} = 1$.

In accordance with the sampling procedure which is carried through a Markov chain Monte Carlo simulation, each configuration appears in the chain of states as dictated by an associated Boltzmann weight. As depicted in Fig. 1, the mathematical operation of convolution acts on an importance-sampled configuration and a series of additional transformations imposed by the neural network lead to the calculation of the probability P_{σ_i} . We therefore interpret P as an observable of the system:

$$\langle P \rangle = \sum_{\sigma} P_{\sigma} p_{\sigma} = \frac{\sum_{\sigma} P_{\sigma} \exp[-\sum_k g^{(k)} S_{\sigma}^{(k)}]}{\sum_{\sigma} \exp[-\sum_k g^{(k)} S_{\sigma}^{(k)}]}. \quad (5)$$

In this framework, the probability P can be extrapolated with histogram reweighting over wide ranges of parameter values $\{g^{(k)}\}$. Specifically for the case of the Ising model, reweighting in terms of inverse temperatures reduces Eq. (4) to:

$$\langle P \rangle_{\beta} = \frac{\sum_{i=1}^N P_{\sigma_i} \exp[-(\beta - \beta_0) E_{\sigma_i}]}{\sum_{i=1}^N \exp[-(\beta - \beta_0) E_{\sigma_i}]}. \quad (6)$$

In Fig. 2, we show the expectation value $\langle P^{(b)} \rangle$ as a function of β for the Ising model with lattice size $L = 128$. The values over this large span of inverse temperatures, depicted by the line, have been obtained by exclusively extrapolating the probabilities from configurations of one Monte Carlo dataset, simulated at $\beta_0 = 0.438$ in the

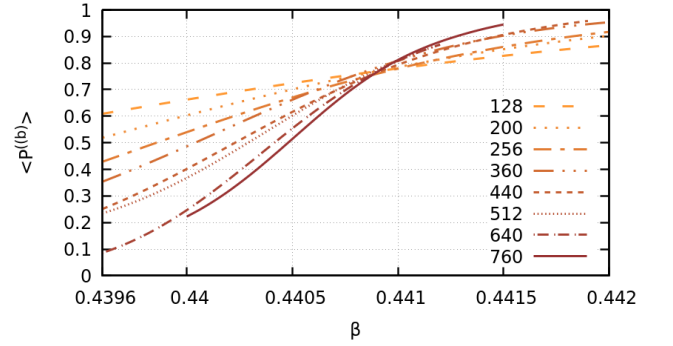


FIG. 3. Reweighted extrapolations of the neural network output probability versus inverse temperature for various lattice sizes.

symmetric phase or $\beta_0 = 0.44$ in the broken-symmetry phase. The results are compared with actual calculations of the average probability, which are acquired from predictions of the convolutional neural network on independent Monte Carlo datasets. We note that the values of reweighting overlap with the ones from actual calculations within statistical errors (App. C), demonstrating the accuracy of the method. We observe that the average probability resembles an order parameter, with values that are consistent with zero and one at different phases. We further note that this order parameter has emerged by features learned on configurations for sets of inverse temperatures which lie beyond a fixed distance from the critical point β_c . The neural network has then fully reconstructed an effective order parameter based on incomplete information and representation of the studied system.

To gain further qualitative insights into the learned features of the neural network, we utilize reweighting to draw the output probability $\langle P^{(b)} \rangle$ for a range of lattice sizes. Previous research (e.g. in Refs. [4, 21]) has evidenced that decision making of a neural network seems

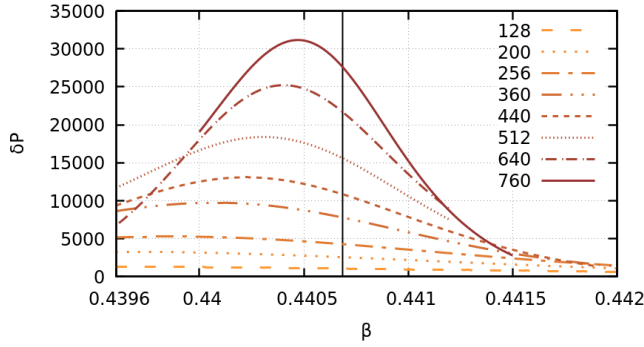


FIG. 4. Fluctuations of the neural network output probability, Eq. 7, for various lattice sizes. The vertical line corresponds to the known critical temperature $\beta_c \approx 0.440687$ of the two-dimensional Ising model.

to rely on some form of devised magnetization function. In Fig. 3 we note that the probabilities for increasing lattice sizes become sharper near the critical point in a way that mimics the behaviour of the magnetization. A natural question is whether it is possible to numerically extract multiple critical exponents based solely on quantities derived from the neural network probability and their reweighted extrapolations. To answer this, we note that near a continuous phase transition and on a lattice of a finite size L , fluctuations such as the magnetic susceptibility χ have a maximum value. A pseudo-critical point $\beta_c^x(L)$ is then associated with the maxima of the fluctuations which in the thermodynamic limit converges to the inverse critical temperature $\lim_{L \rightarrow \infty} \beta_c^x = \beta_c$. Based on the interpretation of the output probability as an effective order parameter and as an observable in the system, we now define its fluctuations weighed by the inverse temperature:

$$\delta P = \beta V (\langle P^2 \rangle - \langle P \rangle^2). \quad (7)$$

As reweighting has been formulated in terms of an arbitrary observable, we use Eq. (4) to estimate the expectation values of both observables $\langle P^2 \rangle$, $\langle P \rangle$ and hence calculate the fluctuations of the probability which are de-

TABLE I. Pseudo-critical points $\beta_c^P(L)$ and maxima of the probability fluctuations δP_{max} for various lattice sizes L of the Ising model.

L	$\beta_c^P(L)$	δP_{max}
128	0.438857(33)	1409(6)
200	0.439536(24)	3308(14)
256	0.439889(18)	5233(24)
360	0.440088(13)	9910(49)
440	0.440261(12)	13138(71)
512	0.440292(10)	18912(99)
640	0.440403(10)	25215(218)
760	0.440465(8)	30841(206)

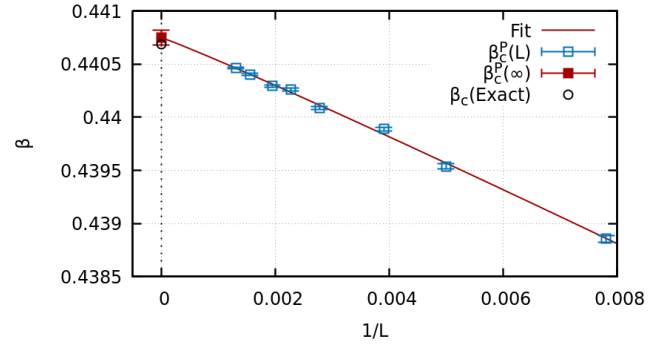


FIG. 5. Inverse critical temperature versus inverse lattice size.

picted in Fig. 4, without including statistical errors. We note that the inverse temperatures where the maximum values of the fluctuations δP are located evidence a scaling behaviour with increasing lattice sizes. This tentatively indicates a convergence towards the known inverse critical temperature of the Ising model $\beta_c \approx 0.440687$, which is depicted by the vertical line. We therefore associate pseudo-critical points $\beta_c^P(L)$ for the values of the maxima δP_{max} (see Tab. I) and we rely on them for our subsequent quantitative analysis.

We now attempt to calculate critical exponents using a finite size scaling analysis without assuming prior knowledge of the critical point. In order to acquire the correlation length exponent ν and an estimate of the inverse critical temperature β_c we note that, due to the divergence of the correlation length in the pseudo-critical region, the reduced temperature can be expressed as:

$$|t| = \left| \frac{\beta_c - \beta_c(L)}{\beta_c} \right| \sim \xi^{-\frac{1}{\nu}} \sim L^{-\frac{1}{\nu}}. \quad (8)$$

Furthermore, based on the resemblance of the neural network output probability with the magnetization we perform a calculation of the magnetic susceptibility exponent γ using the maximum values of the probability fluctuations:

$$\delta P \sim L^{\frac{\gamma}{\nu}}. \quad (9)$$

As visible in Figs. 5 and 6, we fit the data from Tab. I for the pseudo-critical points and the maxima of the probability using Eqs. (8) and (9), respectively. The results of the finite size scaling analysis are given in Tab. II. We note that the acquired estimates for the critical exponents and the inverse critical temperature of the Ising model are within statistical errors of the known values from Onsager's analytical solution. In the error analysis only statistical errors from predictions of the neural network on a finite Monte Carlo dataset were considered.

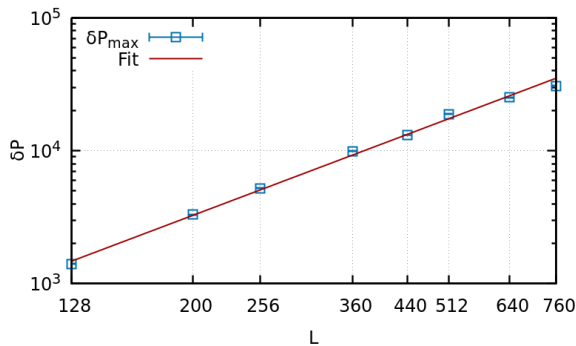


FIG. 6. Probability fluctuations versus lattice size on double logarithmic scale.

IV. CONCLUSIONS

In this paper we introduced histogram reweighting to supervised machine learning. We applied the method to a phase identification task by means of a neural network, uncovered relations between the machine learning output and standard thermodynamic observables of the system, and calculated the inverse critical temperature and critical exponents using a finite size scaling analysis based on the neural network output. Specifically, the results were demonstrated using the phase transition in the two-dimensional Ising model.

Initially, a convolutional neural network is trained on Monte Carlo datasets acquired distantly from the inverse critical temperature to classify phases of the Ising model. The activation function of the output layer is then expressed as a probability that associates a configuration with each phase. Importantly, the output is treated as an observable in the statistical system with an attached Boltzmann weight, enabling its extrapolation with the use of histogram reweighting techniques.

We proceed by interpreting the neural network output probability as an effective order parameter to explore relations with observables in the studied system. We utilize reweighting to draw the output probability for varying lattice sizes and observe within the proximity of the phase transition that it resembles the magnetization. A scaling behaviour emerging from the fluctuations of the output probability is then discovered, which is reminiscent to that of the magnetic susceptibility.

TABLE II. Critical exponents of the Ising model acquired by reweighting quantities of the neural network implementation and comparison with exact values from Onsager's analytical solution.

	β_c	ν	γ/ν
CNN+Reweighting	0.440749(68)	0.95(9)	1.78(4)
Exact	$\ln(1 + \sqrt{2})/2$ ≈ 0.440687	1	$7/4$ $=1.75$

We finally determine the universality class of the Ising model by conducting a finite size scaling analysis based solely on quantities derived from the neural network. The maxima of the probability fluctuations are treated as indicators for pseudo-critical points, leading to the calculation of the correlation length and magnetic susceptibility exponents as well as the inverse critical temperature.

The extension of histogram reweighting to neural networks enables quantitative studies of phase transitions based on a synergistic relation between machine learning and statistical mechanics. Generalizing to multiple histogram reweighting is, in principle, straightforward. The construction of an effective order parameter from a machine learning algorithm could prove useful when a conventional order parameter is absent or unknown. Examples are phenomena that are currently under active investigation, such as topological superconductivity [61], and the finite-temperature phase transition in quantum chromodynamics [62, 63]. Finally, through multi-parameter reweighting, one could explore the extrapolation of machine learning predictions in regions of parameter space where direct sampling with Monte Carlo might not be possible. Such cases potentially include systems with a numerical sign problem [64].

V. ACKNOWLEDGEMENTS

The authors received funding from the European Research Council (ERC) under the European Union's Horizon 2020 research and innovation programme under grant agreement No 813942. The work of GA and BL has been supported in part by the STFC Consolidated Grant ST/P00055X/1. The work of BL is further supported in part by the Royal Society Wolfson Research Merit Award WM170010. Numerical simulations have been performed on the Swansea SUNBIRD system. This system is part of the Supercomputing Wales project, which is part-funded by the European Regional Development Fund (ERDF) via Welsh Government. We thank COST Action CA15213 THOR for support.

Appendix A: Ising Model

We consider the Ising model on a hypercubic two-dimensional square lattice with Hamiltonian:

$$E = -J \sum_{\langle ij \rangle} s_i s_j - h \sum_i s_i, \quad (\text{A1})$$

where $\langle ij \rangle$ denotes a sum over nearest neighbors, J is the coupling constant which is set to one, and h the external magnetic field which is set to zero. The corresponding Boltzmann probability distribution and partition function (1), are given by considering the case $k = 1$, $S^{(1)} = E$ and $g^{(1)} = \beta$ where $\beta = 1/T$ is the inverse temperature.

The system is invariant under a reflection symmetry $\{s_i\} \rightarrow \{-s_i\}$ that can be spontaneously broken. We

define in the vicinity of a continuous phase transition, a dimensionless parameter called the reduced inverse temperature:

$$t = \frac{\beta_c - \beta}{\beta_c}, \quad (\text{A2})$$

where β_c is the critical temperature. The divergence of the correlation length for a system in the thermodynamic limit $\xi = \xi(\beta, L = \infty)$ is given by:

$$\xi \sim |t|^{-\nu}, \quad (\text{A3})$$

with ν the correlation length critical exponent. Another observable of interest is the normalized magnetization:

$$m = \frac{1}{V} \left| \sum_i s_i \right|, \quad (\text{A4})$$

where V is the volume of the system. The magnetic susceptibility is then defined as the fluctuations of the magnetization:

$$\chi = \beta V (\langle m^2 \rangle - \langle m \rangle^2), \quad (\text{A5})$$

and has an associated critical exponent γ , defined via:

$$\chi \sim |t|^{-\gamma}. \quad (\text{A6})$$

The sets of critical exponents determine a universality class. Different systems that belong to the same universality class are governed by the same set of critical exponents. Knowledge of two exponents is sufficient for the calculation of the remaining ones through the use of scaling relations (e.g. see Ref. [57]). The exact results for the two-dimensional Ising model are:

$$\nu = 1, \quad (\text{A7})$$

$$\gamma/\nu = 7/4, \quad (\text{A8})$$

$$\beta_c = \frac{1}{2} \ln(1 + \sqrt{2}) \approx 0.440687. \quad (\text{A9})$$

Appendix B: CNN Architecture

The neural network architecture consists of a two-dimensional convolutional layer with 64 filters of size 2×2 and a stride of 2, supplemented with a rectified linear unit (ReLU) activation function. The result is then passed to a 2×2 max-pooling layer and subsequently to a fully connected layer with 64 ReLU units. The output layer consists of two units with a softmax activation function, with values bound between $[0, 1]$. Configurations in the symmetric phase are labeled as $(1, 0)$ and those in the broken-symmetry phase as $(0, 1)$. We train the neural network until convergence using the Adam algorithm and a mini-batch size of 12. To speed up the learning in small lattices of $L \leq 256$, we choose a learning rate of 10^{-4} and reduce it by a factor of 10 for the remaining sizes.

Appendix C: Bootstrap

The calculation of errors has been conducted with a bootstrap analysis technique [57]. This enables the elimination of any potential bias in the quantity associated with the finiteness of the Monte Carlo generated sample. In particular, each Monte Carlo dataset, comprised of uncorrelated configurations, has been resampled a 1000 times for each lattice size. For each resampled dataset, reweighted extrapolations of the output probability and its fluctuations are acquired in a wide range of temperatures using Eq. (4). The error for the extrapolated probability P at each inverse temperature β is given by equation:

$$\sigma = \sqrt{P^2 - \bar{P}^2}. \quad (\text{C1})$$

where the averages are performed over the bootstrap replicas.

-
- [1] I. J. Goodfellow, Y. Bengio, and A. Courville, *Deep Learning* (MIT Press, Cambridge, MA, USA, 2016) <http://www.deeplearningbook.org>.
 - [2] G. Carleo, I. Cirac, K. Cranmer, L. Daudet, M. Schuld, N. Tishby, L. Vogt-Maranto, and L. Zdeborová, Machine learning and the physical sciences, *Reviews of Modern Physics* **91**, 10.1103/revmodphys.91.045002 (2019).
 - [3] J. Carrasquilla, Machine learning for quantum matter (2020), arXiv:2003.11040 [physics.comp-ph].
 - [4] J. Carrasquilla and R. G. Melko, Machine learning phases of matter, *Nature Physics* **13**, 431 (2017).
 - [5] E. L. van Nieuwenburg, Y.-H. Liu, and S. Huber, Learning phase transitions by confusion, *Nature Physics* **13**, 435 (2017).
 - [6] F. Schindler, N. Regnault, and T. Neupert, Probing many-body localization with neural networks, *Phys. Rev. B* **95**, 245134 (2017).
 - [7] L. Wang, Discovering phase transitions with unsupervised learning, *Phys. Rev. B* **94**, 195105 (2016).
 - [8] W. Hu, R. R. P. Singh, and R. T. Scalettar, Discovering phases, phase transitions, and crossovers through unsupervised machine learning: A critical examination, *Phys. Rev. E* **95**, 062122 (2017).
 - [9] S. J. Wetzel, Unsupervised learning of phase transitions: From principal component analysis to variational autoencoders, *Phys. Rev. E* **96**, 022140 (2017).
 - [10] K. Ch'ng, N. Vazquez, and E. Khatami, Unsupervised machine learning account of magnetic transitions in the

- hubbard model, *Phys. Rev. E* **97**, 013306 (2018).
- [11] P. Broecker, J. Carrasquilla, R. G. Melko, and S. Trebst, Machine learning quantum phases of matter beyond the fermion sign problem, *Scientific Reports* **7**, 8823 (2017).
 - [12] K. Ch'ng, J. Carrasquilla, R. G. Melko, and E. Khatami, Machine learning phases of strongly correlated fermions, *Phys. Rev. X* **7**, 031038 (2017).
 - [13] A. Tanaka and A. Tomiya, Detection of phase transition via convolutional neural networks, *Journal of the Physical Society of Japan* **86**, 063001 (2017), <https://doi.org/10.7566/JPSJ.86.063001>.
 - [14] M. J. S. Beach, A. Golubeva, and R. G. Melko, Machine learning vortices at the kosterlitz-thouless transition, *Phys. Rev. B* **97**, 045207 (2018).
 - [15] P. Ponte and R. G. Melko, Kernel methods for interpretable machine learning of order parameters, *Phys. Rev. B* **96**, 205146 (2017).
 - [16] P. Broecker, F. F. Assaad, and S. Trebst, Quantum phase recognition via unsupervised machine learning (2017), [arXiv:1707.00663 \[cond-mat.str-el\]](https://arxiv.org/abs/1707.00663).
 - [17] C. Wang and H. Zhai, Machine learning of frustrated classical spin models. i. principal component analysis, *Phys. Rev. B* **96**, 144432 (2017).
 - [18] G. Torlai and R. G. Melko, Learning thermodynamics with boltzmann machines, *Phys. Rev. B* **94**, 165134 (2016).
 - [19] P. Suchsland and S. Wessel, Parameter diagnostics of phases and phase transition learning by neural networks, *Phys. Rev. B* **97**, 174435 (2018).
 - [20] N. C. Costa, W. Hu, Z. J. Bai, R. T. Scalettar, and R. R. P. Singh, Principal component analysis for fermionic critical points, *Phys. Rev. B* **96**, 195138 (2017).
 - [21] C. Giannetti, B. Lucini, and D. Vadachino, Machine learning as a universal tool for quantitative investigations of phase transitions, *Nuclear Physics B* **944**, 114639 (2019).
 - [22] J. Greitemann, K. Liu, and L. Pollet, Probing hidden spin order with interpretable machine learning, *Phys. Rev. B* **99**, 060404 (2019).
 - [23] K. Liu, J. Greitemann, and L. Pollet, Learning multiple order parameters with interpretable machines, *Phys. Rev. B* **99**, 104410 (2019).
 - [24] C. Alexandrou, A. Athenodorou, C. Chrysostomou, and S. Paul, Unsupervised identification of the phase transition on the 2d-ising model (2019), [arXiv:1903.03506 \[cond-mat.stat-mech\]](https://arxiv.org/abs/1903.03506).
 - [25] Z. Li, M. Luo, and X. Wan, Extracting critical exponents by finite-size scaling with convolutional neural networks, *Phys. Rev. B* **99**, 075418 (2019).
 - [26] Q. Ni, M. Tang, Y. Liu, and Y.-C. Lai, Machine learning dynamical phase transitions in complex networks, *Phys. Rev. E* **100**, 052312 (2019).
 - [27] W. Zhang, L. Wang, and Z. Wang, Interpretable machine learning study of the many-body localization transition in disordered quantum ising spin chains, *Phys. Rev. B* **99**, 054208 (2019).
 - [28] J. F. Rodriguez-Nieva and M. S. Scheurer, Identifying topological order through unsupervised machine learning, *Nature Physics* **15**, 790 (2019).
 - [29] Y.-T. Hsu, X. Li, D.-L. Deng, and S. Das Sarma, Machine learning many-body localization: Search for the elusive nonergodic metal, *Phys. Rev. Lett.* **121**, 245701 (2018).
 - [30] E. van Nieuwenburg, E. Bairey, and G. Refael, Learning phase transitions from dynamics, *Phys. Rev. B* **98**, 060301 (2018).
 - [31] J. Venderley, V. Khemani, and E.-A. Kim, Machine learning out-of-equilibrium phases of matter, *Phys. Rev. Lett.* **120**, 257204 (2018).
 - [32] R. A. Vargas-Hernández, J. Sous, M. Berciu, and R. V. Krems, Extrapolating quantum observables with machine learning: Inferring multiple phase transitions from properties of a single phase, *Phys. Rev. Lett.* **121**, 255702 (2018).
 - [33] C. Casert, T. Vieijra, J. Nys, and J. Ryckebusch, Interpretable machine learning for inferring the phase boundaries in a nonequilibrium system, *Phys. Rev. E* **99**, 023304 (2019).
 - [34] L. Onsager, Crystal statistics. i. a two-dimensional model with an order-disorder transition, *Phys. Rev.* **65**, 117 (1944).
 - [35] J. Liu, Y. Qi, Z. Y. Meng, and L. Fu, Self-learning monte carlo method, *Phys. Rev. B* **95**, 041101 (2017).
 - [36] L. Huang and L. Wang, Accelerated monte carlo simulations with restricted boltzmann machines, *Phys. Rev. B* **95**, 035105 (2017).
 - [37] L. Wang, Exploring cluster monte carlo updates with boltzmann machines, *Phys. Rev. E* **96**, 051301 (2017).
 - [38] Y. Nagai, H. Shen, Y. Qi, J. Liu, and L. Fu, Self-learning monte carlo method: Continuous-time algorithm, *Phys. Rev. B* **96**, 161102 (2017).
 - [39] X. Y. Xu, Y. Qi, J. Liu, L. Fu, and Z. Y. Meng, Self-learning quantum monte carlo method in interacting fermion systems, *Phys. Rev. B* **96**, 041119 (2017).
 - [40] H. Shen, J. Liu, and L. Fu, Self-learning monte carlo with deep neural networks, *Phys. Rev. B* **97**, 205140 (2018).
 - [41] C. Chen, X. Y. Xu, J. Liu, G. Batrouni, R. Scalettar, and Z. Y. Meng, Symmetry-enforced self-learning monte carlo method applied to the holstein model, *Phys. Rev. B* **98**, 041102 (2018).
 - [42] S. Li, P. M. Dee, E. Khatami, and S. Johnston, Accelerating lattice quantum monte carlo simulations using artificial neural networks: Application to the holstein model, *Phys. Rev. B* **100**, 020302 (2019).
 - [43] Y. Nagai, M. Okumura, K. Kobayashi, and M. Shiga, Self-learning hybrid monte carlo: A first-principles approach (2019), [arXiv:1909.02255 \[cond-mat.mtrl-sci\]](https://arxiv.org/abs/1909.02255).
 - [44] T. Song and H. Lee, Accelerated continuous time quantum monte carlo method with machine learning, *Phys. Rev. B* **100**, 045153 (2019).
 - [45] Y. Nagai, M. Okumura, and A. Tanaka, Self-learning monte carlo method with behler-parrinello neural networks, *Phys. Rev. B* **101**, 115111 (2020).
 - [46] Y. Liu, W. Wang, K. Sun, and Z. Y. Meng, Designer monte carlo simulation for the gross-neveu-yukawa transition, *Phys. Rev. B* **101**, 064308 (2020).
 - [47] E. M. Inack, G. E. Santoro, L. Dell'Anna, and S. Pilati, Projective quantum monte carlo simulations guided by unrestricted neural network states, *Phys. Rev. B* **98**, 235145 (2018).
 - [48] S. Pilati, E. M. Inack, and P. Pieri, Self-learning projective quantum monte carlo simulations guided by restricted boltzmann machines, *Phys. Rev. E* **100**, 043301 (2019).
 - [49] K.-W. Zhao, W.-H. Kao, K.-H. Wu, and Y.-J. Kao, Generation of ice states through deep reinforcement learning, *Phys. Rev. E* **99**, 062106 (2019).
 - [50] D. Wu, L. Wang, and P. Zhang, Solving statistical mechanics using variational autoregressive networks, *Phys.*

- Rev. Lett. **122**, 080602 (2019).
- [51] F. Noé, S. Olsson, J. Köhler, and H. Wu, Boltzmann generators: Sampling equilibrium states of many-body systems with deep learning, *Science* **365**, 10.1126/science.aaw1147 (2019).
 - [52] K. Zhou, G. Endrödi, L.-G. Pang, and H. Stöcker, Regressive and generative neural networks for scalar field theory, *Phys. Rev. D* **100**, 011501 (2019).
 - [53] M. S. Albergo, G. Kanwar, and P. E. Shanahan, Flow-based generative models for markov chain monte carlo in lattice field theory, *Phys. Rev. D* **100**, 034515 (2019).
 - [54] G. Kanwar, M. S. Albergo, D. Boyda, K. Cranmer, D. C. Hackett, S. Racanire, D. J. Rezende, and P. E. Shanahan, Equivariant flow-based sampling for lattice gauge theory (2020), arXiv:2003.06413 [hep-lat].
 - [55] A. M. Ferrenberg and R. H. Swendsen, New monte carlo technique for studying phase transitions, *Phys. Rev. Lett.* **61**, 2635 (1988).
 - [56] A. M. Ferrenberg and R. H. Swendsen, Optimized monte carlo data analysis, *Phys. Rev. Lett.* **63**, 1195 (1989).
 - [57] M. E. J. Newman and G. T. Barkema, *Monte Carlo methods in statistical physics* (Clarendon Press, Oxford, 1999).
 - [58] U. Wolff, Collective monte carlo updating for spin systems, *Phys. Rev. Lett.* **62**, 361 (1989).
 - [59] M. Abadi *et al.*, TensorFlow: Large-scale machine learning on heterogeneous systems (2015), software available from tensorflow.org.
 - [60] F. Chollet *et al.*, Keras, <https://keras.io> (2015).
 - [61] M. Sato and Y. Ando, Topological superconductors: a review, *Reports on Progress in Physics* **80**, 076501 (2017).
 - [62] S. Borsányi, Z. Fodor, C. Hoelbling, S. D. Katz, S. Krieg, C. Ratti, and K. K. Szabó, Is there still any tc mystery in lattice qcd? results with physical masses in the continuum limit iii, *Journal of High Energy Physics* **2010**, 73 (2010).
 - [63] A. Bazavov, T. Bhattacharya, M. Cheng, C. DeTar, H.-T. Ding, S. Gottlieb, R. Gupta, P. Hegde, U. M. Heller, F. Karsch, E. Laermann, L. Levkova, S. Mukherjee, P. Petreczky, C. Schmidt, R. A. Soltz, W. Soeldner, R. Sugar, D. Toussaint, W. Unger, and P. Vranas (HotQCD Collaboration), Chiral and deconfinement aspects of the qcd transition, *Phys. Rev. D* **85**, 054503 (2012).
 - [64] G. Aarts, Introductory lectures on lattice qcd at nonzero baryon number, *Journal of Physics: Conference Series* **706**, 022004 (2016).